Springer

KSME

Journal of Mechanical Science and Technology 27 (9) (2013) 2845~2856
www.springerlink.com/content/1738-494x
DOI 10.1007/s12206-013-0733-3

Influence of gas turbine specification and integration option on the performance of integrated gasification solid oxide fuel cell/gas turbine systems with CO_2 capture †

Ji Ho Ahn[1], Sung Ku Park[1], Tong Seop Kim[2,*]

[1]*Graduate School, Inha University, Incheon 402-751, Korea*
[2]*Dept. of Mechanical Engineering, Inha University, Incheon 402-751, Korea*

(Manuscript Received September 17, 2012; Revised January 21, 2013; Accepted March 25, 2013)

Abstract

We investigated key design features of the integrated gasification solid oxide fuel cell/gas turbine (IG-SOFC/GT) system including carbon dioxide capture. Two different types of system configurations that depend on the carbon dioxide capture scheme (pre- and oxy-combustion captures) were examined. Research focus was given to the effect of the gas turbine specification on the performance of the entire system. IG-SOFC/GT systems using two different gas turbines were analyzed, and their performances were compared. A parametric analysis was carried out to further understand the performance comparison. We found that the net system efficiency was not very sensitive to the turbine inlet temperature and the pressure ratio. As a result, similar net efficiencies were observed between the systems using two gas turbines with quite different specifications. In addition, a revision of the system layout was investigated and it was found that the power capacity of the system could be increased and the system efficiency could also be slightly enhanced by supplying nitrogen separated from the air separation unit to the fuel cell rather than to the gas turbine combustor.

Keywords: Gas turbine; Solid oxide fuel cell; Coal gasification; Pre-combustion CO_2 capture; Oxy-combustion CO_2 capture; Net efficiency

1. Introduction

The integrated gasification combined cycle (IGCC) is an effective technology to generate electric power from coal with a low environmental impact. Various studies have been performed recently regarding design options [1], operating characteristics [2, 3], the effects of syngas properties [4], and CO_2 capture [5-7]. Solid oxide fuel cells (SOFCs) are also recognized as promising future power sources. SOFCs are expected to be useful both in small distributed power generation systems and in large power stations [8, 9]. Using coal as the fuel for SOFCs could also be a good option to consume coal cleanly and efficiently. Furthermore, the hybridization of SOFCs with gas turbine s (GTs) is expected to upgrade system efficiency and environmental friendliness. Small-scale SOFC/GT hybrid systems have been actively researched, and improved efficiency compared to SOFC efficiency has been confirmed in a field test [10]. The number of fundamental studies of the use of coal in SOFCs and SOFC/GT hybrid systems has increased rapidly in recent years [11-14], and various system configurations have been suggested.

Recently proposed diverse power generation systems adopting CO_2 capture are based on one of the three capture technologies: pre-, post-, and oxy-combustion capture [15, 16]. In coal power plants using gasification technology such as IGCC, pre-combustion capture is preferred because it can be added to the gasification process. The usefulness of oxy-fuel combustion technology has also been highlighted recently. Flue gas from the combustion of fuel with pure oxygen consists mainly of CO_2 and H_2O. Therefore, a rather simple mechanical CO_2 separation scheme such as condensation and subsequent separation of gaseous CO_2 can be used instead of more complex and energy-consuming processes such as absorption-based separation schemes. Various power plant systems adopting oxy-combustion technology have been devised, and their performance expectations have been published recently [14, 17-20]. In particular, a recent study suggested the use of oxy-combustion in a coal gasification plant combining a gas turbine and the SOFC [14]. In the oxygen separation industry, particular attention is being given to the development of membrane technologies which consume much less electric power than conventional methods [21]. The applicability of an ion transport membrane (ITM) that separates oxygen from the fuel cell cathode exit air in SOFC/GT combined systems has been examined recently [14, 22].

*Corresponding author. Tel.: +82 32 860 7307, Fax.: +82 32 868 1716
E-mail address: kts@inha.ac.kr
† Recommended by Associate Editor Yong-Tae Kim

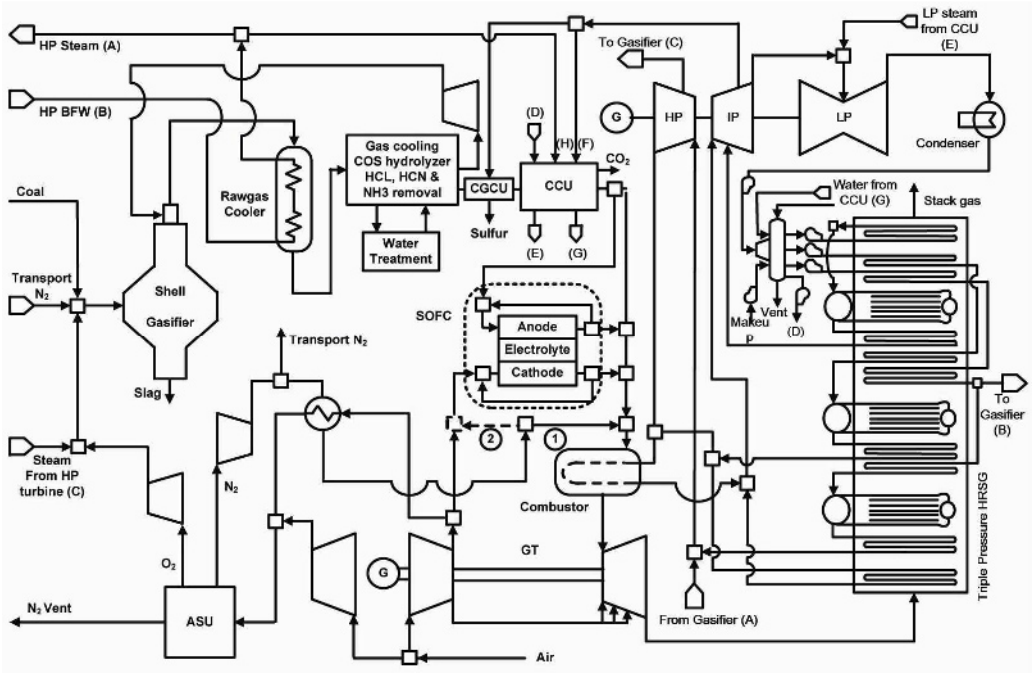

Fig. 1. Schematic diagram of IG-SOFC/GT system with pre-combustion CO_2 capture.

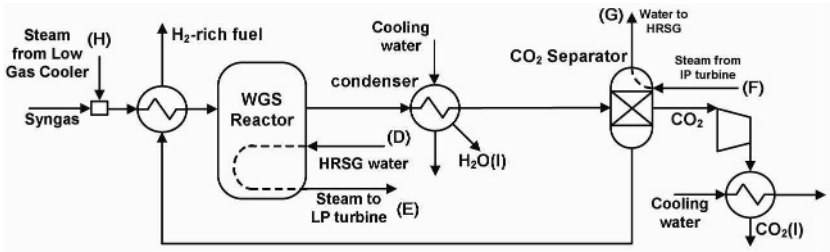

Fig. 2. Schematic diagram of pre-combustion CO_2 capture unit.

The aforementioned research and development trends show that the combination of the SOFC with a gas turbine, and the least energy-consuming CO_2 capture, are the two core concepts for future coal power plant technology. A recent study [14] suggested integrated gasification SOFC/GT systems that combine the two concepts. In Ref. [14], several system configurations were devised, and their performances were analyzed and compared with the baseline IGCC. The significance of the study is that the proposed IG-SOFC/GT systems share the structural backbone of the currently available IGCC plant, and yet provide much higher efficiency than the IGCC. Considering the thermodynamic advantage of the proposed systems, follow-up studies are required to better understand performance characteristics and to develop performance improvements. In this regard, the effects of various design factors on system performance needs to be examined. In particular, the impact of gas turbine specifications should be investigated because the specifications of a gas turbine have a very wide selection range in terms of power and efficiency.

Accordingly, we examined the effects of the gas turbine specifications on the performance of IG-SOFC/GT systems. IG-SOFC/GT systems using two different gas turbines were analyzed, and their performances were compared. A parametric analysis was carried out to explain the results of the performance comparison. In addition, a revision of the system layouts was considered in order to further enhance system performance.

2. System configuration

The major sub-systems of the IG-SOFC/GT systems in this study are a gasification block, a gas turbine combined cycle power block, a SOFC power block, and CO_2 capture and separation units (CCU and CSU). Two different system layouts were analyzed in this study: pre- and oxy-combustion capture-based systems. The cathode inlet air temperature of the SOFC should not be significantly lower than the cell stack temperature for reliability. Several schemes were compared in Ref. [14], and the method of recirculating the cathode exit air to the inlet was found to be superior in terms of system efficiency. Accordingly, the recirculation scheme described in Ref. [14] was adopted in this study as shown in Fig. 1 (note the flow

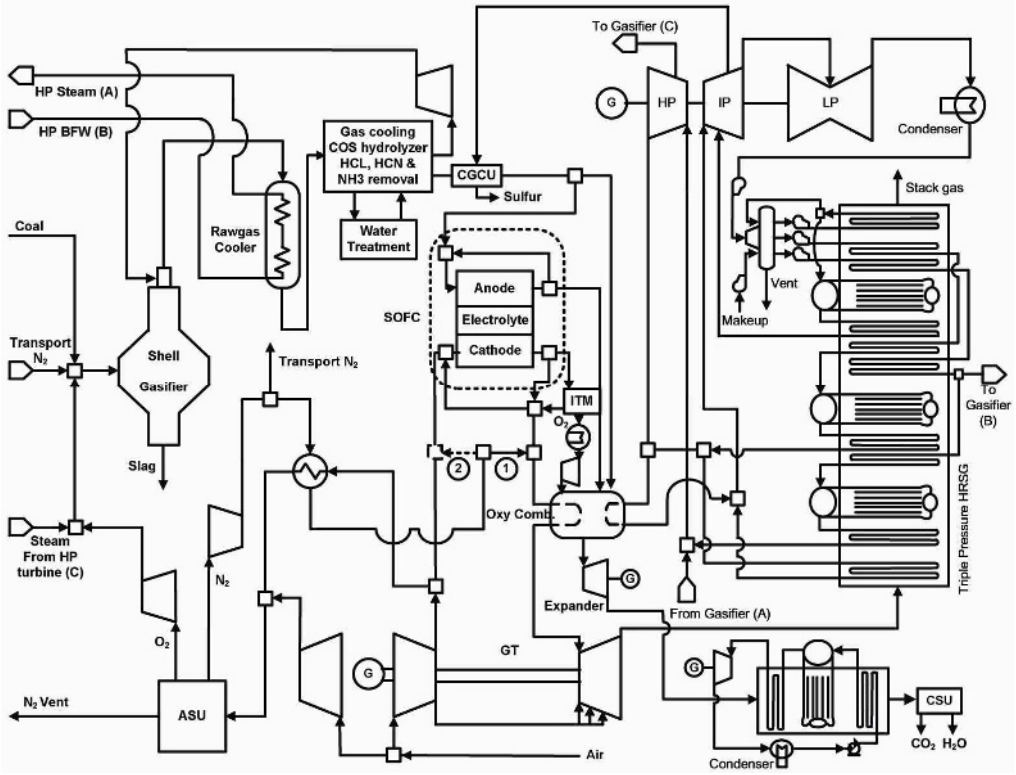

Fig. 3. Schematic diagram of IG-SOFC/GT system with oxy-combustion CO_2 capture.

streams around the SOFC), and also in Fig. 3.

First, we describe the pre-combustion capture-based system shown in Fig. 1. Air is first compressed in the gas turbine compressor and is then fed to the SOFC. In the SOFC, fuel is supplied and reacts with the air electrochemically, thereby generating power. Both the unreacted fuel in the SOFC and the additionally supplied fuel are burned in the combustor. The purpose of the additional fuel supply is to meet the required turbine inlet temperature of the gas turbine. The high pressure and temperature gas expands in the turbine and the resulting flue gas drives the steam bottoming cycle.

The gasifier is an oxygen-blown type and needs a cryogenic air separation unit (ASU). The air to the ASU is partially supplied by the compressor of the gas turbine and partially supplied by a separate compressor. The separated oxygen is supplied to the gasifier as an oxidizer. Part of the nitrogen separated from the ASU is directed to the power block and some is used for coal transportation. With regard to the supply of the nitrogen to the power block, two cases were examined. In the reference case, indicated by ①, the nitrogen is directed to the combustor. The alternative, indicated by ②, is to mix the nitrogen with the cathode inlet air of the SOFC. We first examine the reference case. The alternative case will be treated in section 4.3. The steam required in the gasifier is supplied by the high pressure steam turbine. The high temperature raw gas produced in the gasifier is cooled in the raw gas cooler by the high pressure water from the HRSG. Part of the steam from the intermediate pressure steam turbine is used in the conversion process of the cold gas cleanup unit (CGCU), where sulfur is recovered. The pre-combustion CCU is shown in Fig. 2 and is located in the syngas line between the gasifier and the combustor. The syngas from the gasifier and part of the high pressure steam generated at the raw gas cooler react, converting CO into CO_2 and H_2 through a water-gas shift reaction. The cooling water for the exothermic shift reaction is supplied from the steam cycle and is returned to the low pressure steam turbine as vapor. The water vapor in the converted syngas is extracted after condensation, and the CO_2-rich gas in the converted syngas is extracted at the separator. The adopted CO_2 separator is the Selexol process, which is an absorption-based separation process using a physical solvent and is suitable for high volumes of syngas stream [6, 7]. The process requires heat for the solvent regeneration: part of the steam extracted from the intermediate pressure steam turbine supplies heat to the regenerator and returns to the HRSG as liquid. The captured CO_2 is compressed to a high pressure and cooled to liquid for storage or transportation. The resulting H_2-rich fuel is pre-heated by the incoming syngas, and is then supplied to the combustor. Two gas turbines in different technology levels (G and E-class engines) were used, and a typical triple-pressure steam bottoming cycle was adopted.

Fig. 3 shows an IG-SOFC/GT system using oxy-fuel combustion capture. The key feature of the system is that the remaining fuel from the SOFC is burned with the oxygen extracted from the cathode exit gas. The syngas is directly supplied to the anode of the SOFC, and the unreacted fuel in

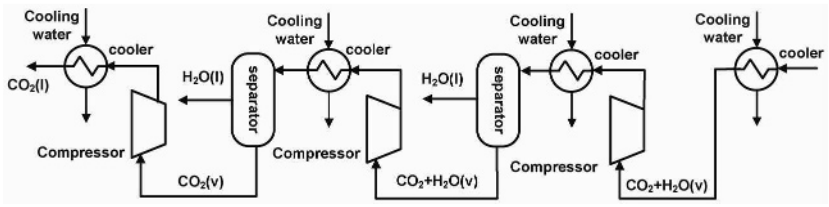

Fig. 4. Schematic diagram of CO_2 separation unit.

the anode is supplied to the oxy-combustor. Part of the cathode exit gas is supplied to the ITM, which separates oxygen from the gas. An ITM produces high-purity oxygen from air via a partial pressure difference across a ceramic membrane. ITM technology requires high operating pressure (about 7 to 35 bar) and temperature (800 to 900 ^oC) [23, 24]. The operating conditions of the SOFC in our system configuration (over 10 bar and 900 ^oC) are quite suitable for the use of the ITM. With an ITM, extremely pure oxygen (over 99%) can be obtained [25].

The ITM does not require power consumption. However, the oxygen separated from the ITM is at the ambient pressure and should be compressed up to the combustor pressure. To minimize the compression power, the oxygen was cooled down to a near ambient temperature before being compressed. Some syngas is supplied to the combustor to meet the required turbine and expander inlet temperatures. The oxygen-depleted gas from the ITM is mixed with the cathode exit gas. Some of the mixed gas is recirculated to the cathode inlet to meet the cathode inlet temperature. The remaining gas is heated to the required turbine inlet temperature and then drives the turbine. The concept of the indirect heating of turbine inlet gas in the oxy-combustor was taken from the layout of a previously suggested oxy-fuel combustion based power generation system [22], where the turbine inlet temperature was below 1000^oC. In the present study, the required turbine inlet temperature ranges from 1100 to 1500^oC and thus the combustor material problem could be a technical barrier. However, because this study aimed to present thermodynamic feasibility of incorporating oxy-fuel combustion in the IG-SOFC/GT system, we performed the cycle simulation under the assumption that future advances in material and combustor design technology could realize the design concept. The high pressure combustion gas from the oxy-combustor consists of CO_2 and H_2O, and expands in a separate expander to the atmospheric pressure, thus producing additional power output. To fully utilize the high temperature of the expander exit gas, a single pressure heat recovery steam turbine cycle is installed, and additional power is generated. The final flue gas is fed to the carbon separation unit (CSU), which uses multiple compressions with intercooling as shown in Fig. 4. Liquid H_2O is extracted in the middle of the process, and the final gaseous phase containing high-purity CO_2 is further compressed and cooled for storage.

3. Modeling and analysis

The entire system was modeled using ASPEN HYSYS [26]. ISO ambient air conditions (1.013 bar, 15^oC, 60% relative humidity) were used in the analysis.

3.1 Gasification process

The gasification process was modeled with reference to Ref. [27]. Table 1 shows the coal properties and major operating conditions of the gasifier, taken from Ref. [27]. The gasifier was modeled as a two-zone reactor with combustion and equilibrium reaction zones. The raw gas was cooled by high-pressure water from the HRSG. We assumed that sulfur was removed from the CGCU. The details of the CGCU were not modeled, but its major impact on the energy balance of the entire system (i.e., the steam supply from the intermediate pressure steam turbine) was included. The percentage of steam extracted from the IP steam turbine was set at 8.5%, based on Ref. [27]. More modeling details can be found in Ref. [14]. The simulated syngas consists of 64.3% CO, 29.4% H_2, 4.0% N_2, and others by volume; these values are quite similar to the reference data in Ref. [27], as validated in Ref. [14].

3.2 Air separation unit

A cryogenic ASU was modeled with reference to [28]. The ASU consumes electrical power for gas compression and liquid pumping. The total power consumed in the air separation process was calculated as follows:

$$\dot{W}_{ASU} = \left(\dot{W}_{MAC} + \dot{W}_{BAC} + \dot{W}_{C,\mathrm{O}_2} + \dot{W}_{P,O_2} + \dot{W}_{C,\mathrm{N}_2}\right)/\eta_{mo}\,. \quad (1)$$

The oxygen and nitrogen compressors and the main air compressor are shown in Fig. 1. The other components (the booster air compressor and pumps) are included in the device denoted by "ASU", the details of which are described in Ref. [14]. The validation of the ASU model can also be found in Ref. [14]: the calculated specific power consumption (power per unit oxygen generation) is in very good agreement (less than 1% discrepancy) with data from Ref. [28] for a practical oxygen purity range. The purities of separated nitrogen and oxygen in the present study were set at 98.9% and 95.0%, respectively. The integration degree, which is defined as the

Table 1. Main parameters of IG-SOFC/GT system.

Gasification process		
Coal composition (weight %, dry)		
C	71.72	
H_2	5.06	
N_2	1.41	
Cl	0.33	
S	2.82	
Ash	10.91	
O_2	7.75	
Higher heating value of coal (kJ/kg)	30531.1	
Gasifier exit temperature (°C)	1006.5	
Gasifier exit pressure (kPa)	2430.4	
Air separation unit		
N_2 and O_2 purity (%)	98.9/95.0	
Integration degree (%)	50.0	
Nitrogen dilution level (%)	63.83	
Oxygen delivery pressure to gasifier (kPa)	3254	
N_2delivery pressure to GT combustor (kPa)	2068	
CO_2 capture unit of the pre-combustion capture		
Steam-to-CO ratio (by mole)	1.5	
CO_2 delivery pressure (bar)	150	
CO_2 delivery temperature (°C)	40	
CO_2 separation efficiency of the separator (%)	95	
SOFC		
Stack temperature (°C)	900	
Cathode inlet temperature (°C)	700 °C	
Steam to carbon ratio	3	
Fuel utilization factor	0.7	
DC-to-AC conversion efficiency (%)	93.0	
Gas Turbine	G-class	E-class
Inlet air flow rate (kg/s)	544.3	294.4
Turbine inlet temperature (°C)	1500	1145
Turbine rotor inlet temperature (°C)	1417	1105
Compressor pressure ratio	19.1	12.6
Coolant fraction relative to inlet air (%)	16.8	12.6
Compressor polytropic efficiency (%)	90.8	89.7
Turbine polytropic efficiency (%)	90.5	86.6
Mechanical efficiency (%)	99.5	98.5
Generator efficiency (%)	98.5	97.5
HRSG and steam turbine		
Max. HP/IP turbine inlet temperature (°C)	565.5	
LP turbine inlet temperature (°C)	250.0	
HP/IP/LP pressure (kPa)	12,411/2,358/241.3	
Condensing pressure (kPa)	5	
HP/IP/LP pinch temperature difference (°C)	35/40/10	
HP/IP/LP isentropic efficiency (%)	87.8/91.3/92.1	
Pump isentropic efficiency (%)	80.0	
Oxy-combustion capture		
ITM operating temperature (°C)	900	
Expander inlet temperature (°C)	910	
Additional steam turbine cycle		
Steam pressure (bar)	30	
Steam temperature (°C)	450	
Turbine isentropic efficiency (%)	88	
Condensing pressure (kPa)	5	
CO_2 separation unit		
CO_2 delivery pressure (bar)	150	
CO_2 delivery temperature (°C)	40	
Others		
Pressure losses (%)	0.5 to 5.0	
Motor efficiency (%)	95.0	

ratio of ASU air supplied by the gas turbine compressor to the total ASU air requirement, was set at 50% [27]. The nitrogen dilution level, which is defined as the ratio of the nitrogen supplied to the gas turbine combustor to the total amount of separated nitrogen from the ASU, was set at 63.8% [27]. The major operating parameters are listed in Table 1.

3.3 Pre-combustion CO_2 capture

The pre-combustion capture process is shown in Fig. 2. The water-gas shift reaction was assumed to occur at an equilibrium condition. The steam-to-CO ratio was assumed to be 1.5, and the CO to CO_2 conversion ratio was estimated to be 94.7% according to equilibrium reaction. The Selexol process (the CO_2 separator shown in Fig. 2) was not modeled in detail, but its impact on the performance of the entire system was considered via the inclusion of its electric power consumption and thermal energy consumption (steam supply) for the solvent regeneration. An average electric power consumption of 109.15 kW/kg/s, as cited in Ref. [29], was used. The ratio of steam extracted from the intermediate pressure steam turbine for solvent regeneration was determined with reference to Ref. [6]. The steam condenses at the CO_2 separator and returns to the deaerator of the HRSG. The CO_2 separation efficiency was assumed to be 95%. In addition to the power consumption at the CO_2 separator, the CCU also requires some power consumption for CO_2 compression and water pumping. The major parameters of the capture process are listed in Table 1. The total CCU power consumption is expressed as follows:

$$\dot{W}_{CC} = \left(\dot{W}_{S,\mathrm{CO_2}} + \dot{W}_{C,\mathrm{CO_2}} + \sum \dot{W}_{P,\mathrm{H_2O}}\right)/\eta_{mo}. \quad (2)$$

3.4 Solid oxide fuel cell

The cell operating temperature and the cathode inlet air temperature were set at 900 C and 700°C, respectively. The major operating parameters of the SOFC system are listed in Table 1. Hydrogen and carbon monoxide from the syngas participate in the following electrochemical reactions at the SOFC, producing direct current:

$$\mathrm{H_2} + \frac{1}{2}\mathrm{O_2} \rightarrow \mathrm{H_2O}, \quad \mathrm{CO} + \frac{1}{2}\mathrm{O_2} \rightarrow \mathrm{CO_2}. \quad (3)$$

Since the operating temperature of SOFC is high, steam reforming and water gas shift inside the fuel cell stack were taken into account. All the reactions inside the fuel cell were assumed to take place at equilibrium. The fuel utilization factor inside the fuel cell stack (the ratio of consumed hydrogen and carbon monoxide) was assumed to be 0.7. The anode exit gas consists of the remaining H_2 and CO, and non-reacting syngas components. The reference cell voltage at the ambient pressure was assumed to be 0.7 V, and a correction due to a change in the operating pressure of the cell [30] was applied as follows:

$$V = V_{ref} + \Delta V = V_{ref} + \left(RT/4F\right)\cdot \ln\left(P/P_{ref}\right). \quad (4)$$

The fuel cell power was calculated using the following equation, where the DC-to-AC conversion efficiency and the auxiliary power consumption in the accessory parts of the SOFC (such as the anode and cathode recirculation blowers) were considered.

$$\dot{W}_{SOFC} = \dot{W}_{SOFC,DC}\cdot\eta_{conv} - \dot{W}_{aux,SOFC}$$

where $\dot{W}_{SOFC,DC} = V\cdot\left(\dot{n}_{H_2} + \dot{n}_{CO}\right)\cdot 2F$. (5)

3.5 Gas turbine combined cycle

Two different gas turbines were used. The first is a G-class gas turbine that represents state-of-the-art technology. Its turbine inlet temperature and pressure ratio were 1500°C and 19.1, respectively. The second is an E-class gas turbine with a turbine inlet temperature of 1145°C and pressure ratio of 12.6. Of course, the former has considerably higher efficiency and specific power (power output divided by inlet air flow rate). The two gas turbines were modeled to reproduce the performance of the engine described in Refs. [27, 31, 32]. A stage-by-stage calculation of the turbine, including mixing of the mainstream gas with cooling air, was performed. The coolant was extracted from the compressor exit. Steam cooling of the combustor in case of the G-class engine due to its high combustion temperature was modeled as indicated in Ref. [27]. It is not adopted in the E-class engine. The net power output of the gas turbine was calculated as follows:

$$\dot{W}_{GT} = \left(\dot{W}_T - \dot{W}_C/\eta_m\right)\cdot\eta_{gen}. \quad (6)$$

The steam bottoming cycle is a triple pressure type that was modeled according to Ref. [27]. The steam turbine calculation was divided into three sections (high, intermediate, and low pressure turbines), and the power output was calculated as follows:

$$\dot{W}_{ST} = \left(\dot{W}_{T,HP} + \dot{W}_{T,IP} + \dot{W}_{T,LP}\right)\cdot\eta_{gen} - \dot{W}_{aux,ST}. \quad (7)$$

The auxiliary power consumption is the power required for pumping liquid water in the steam turbine cycle. The various interactions between the steam cycle and the gasifier block including the CO_2 capture process were considered, as described in section 2. The major operating parameters of the gas turbine combined cycle are listed in Table 1. The maximum HP and IP inlet steam temperature was set to 565.5°C [27]. If the gas turbine exit temperature was too low to raise the steam temperature to this maximum value, the steam temperature was set to 10°C below the gas temperature.

3.6 Components for oxy-combustion capture

The following additional models were used for the system adopting the oxy-combustion capture (Fig. 3). Generation of pure oxygen at the ITM was assumed. Both the gas expander and the additional steam cycle produced extra power. Their specifications are listed in Table 1. A higher expander inlet temperature would allow greater power output. However, this decreases net system efficiency because the increase in the total fuel supply prevails over the power increase [14]. Therefore, the expander inlet temperature was set at 910°C, which is 10°C higher than the temperature of the cathode exit gas supplied to the combustor [14]. The HRSG exit gas was cooled to 70°C before it entered the first compressor of the CSU to minimize the compression power. The inlet temperatures of the second and third compressors of the CSU were set at 60°C. The final state of the liquid CO_2 was the same as in the pre-combustion capture. The power consumptions for gas compression and water pumping in the CO_2 capture process (Fig. 4) were taken into account.

3.7 Net performance

The net cycle efficiency was calculated as follows:

$$\eta_{net} = \frac{\dot{W}_{net}}{\left(\dot{m}\cdot HHV\right)_{coal}}. \quad (8)$$

The net power output of the IG-SOFC/GT system was calculated as follows :

pre-combustion :

$$\dot{W}_{net} = \dot{W}_{SOFC} + \dot{W}_{GT} + \dot{W}_{ST} - \dot{W}_{sys,aux}$$

oxy-combustion :

$$\dot{W}_{net} = \dot{W}_{SOFC} + \dot{W}_{GT} + \dot{W}_{ST} + \dot{W}_{exp} + \dot{W}_{ST2} - \dot{W}_{sys,aux}$$

where $\dot{W}_{sys,aux} = \dot{W}_{ASU} + \dot{W}_{misc} + \dot{W}_{CC}$. (9)

The major portion of the system auxiliary power includes power consumption due to the ASU and the CO_2 capture process. The miscellaneous power includes all other power consumption sources such as the coal compression power, the syngas recirculation power, and the oxygen compression power after the ITM (only in the oxy-combustion system).

4. Results and discussion

The impact of CO_2 capture in the IG-SOFC/GT system will be described first. Then, the impact of using different gas turbines will be discussed. Finally, the impact of modifying the two system layouts by changing the location of the nitrogen supply in the power block will be discussed.

4.1 General trend

For both cases using the G-class and E-class gas turbines, three IG-SOFC/GT systems were simulated. The base case is a system without CO_2 capture; i.e., the system shown in Fig. 1 except for the pre-combustion capture. Table 2 shows the

results of the simulations. The results for the G-class gas turbine case are almost the same as in the previous study [14]. Fig. 5 shows the power splits between the gas turbine, the steam turbine, the SOFC, and the additional expander and steam turbine. The oxy-combustion capture exhibits less efficiency penalty (i.e. higher net efficiency) than the pre-combustion capture, while its net power output is relatively less. Details of the performance difference between the two schemes may be referred to Ref. [14]. Here, we will briefly summarize the trend.

The major performance penalty in the pre-combustion capture is the reduced steam power generation caused by the heat supply from the steam cycle to the capture process and the additional power requirement at the capture process. In the system using oxy-combustion capture, the gas turbine power output is considerably less than in the non-captured case because the turbine flow rate is smaller: the oxy-combustor exit gas is supplied to the expander. The gas turbine exit temperature of the oxy-combustion case was lower than those in the other cases because the compositions of the exhaust gasses are quite different from those of other cases. This results in less steam turbine power output than in the non-captured case. However, the power is still larger than in the pre-combustion case. The main advantage of adopting oxy-combustion capture is the power production by the expander and the additional steam turbine. The sum of the two powers almost amounts to one-half of the main steam turbine power. Nevertheless, the net power output is less than in the system using the pre-combustion capture. However, the significantly reduced total coal supply results in noticeably higher net efficiency.

The effects of CO_2 capture on system performance of the E-class gas turbine based system were turned out to be similar to those of the G-class gas turbine based system. Furthermore, the net efficiencies are nearly the same in the corresponding systems using the two different gas turbines. A detailed analysis on the reason for the similar efficiencies will be treated in the next section.

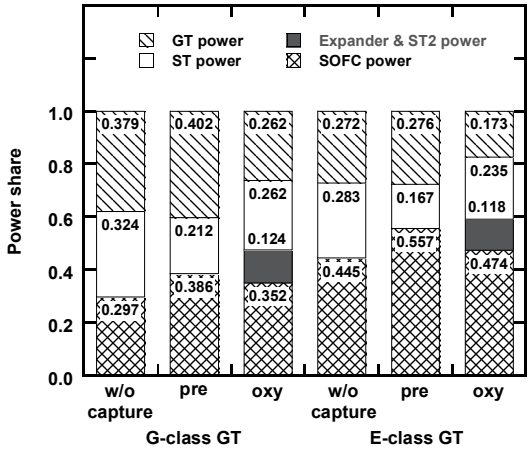

Fig. 5. Power share of IG-SOFC/GT system.

4.2 Influence of gas turbine specification

The major difference between the system using the E-class gas turbine and the system using the G-class gas turbine is the power contribution of the gas turbine. It is considerably lower in the system using the E-class engine (See Fig. 5). Regardless of the existence of the CO_2 capture, the power shares of the gas turbine and the steam turbine are lower (i.e., the power share of the SOFC is greater) in comparison to the G-class case. The power share of the SOFC is around one-half on average in the E-class cases, while it is around one-third on average in the G-class cases. Of course, the system power output is smaller in the E-class cases because its gas turbine air flow is less: the air flow ratio is 54% (see Table 1 for a comparison of the air flow rates). The lower specific power of the entire system using the E-class gas turbine is due to the relatively lower specific power of the gas turbine itself compared to the G-class gas turbine. A gas turbine with a lower turbine inlet temperature has a lower specific power in general

Table 2. Performance summary of IG-SOFC/GT systems: nitrogen supply to the combustor.

	G-class gas turbine			E-class gas turbine		
CO_2 capture method	w/o capture	Pre-comb.	Oxy- comb.	w/o capture	Pre-comb.	Oxy-comb.
Gross power (MW)	782.7	752.9	678.0	346.4	346.1	328.9
GT power (MW)	296.6	303.0	177.6	94.1	95.5	57.0
Main ST power (MW)	253.4	159.5	177.9	98.1	57.7	77.2
Additional ST power (MW)	-	-	16.6	-	-	9.8
CO_2 expander power (MW)	-	-	67.5	-	-	28.9
SOFC power (MW)	232.7	290.4	238.4	154.2	192.9	156.0
Auxiliary power (MW)	-84.0	-134.2	-138.1	-37.4	-61.4	-64.85
ASU power (MW)	-67.0	-78.0	-58.8	-29.8	-35.6	-28.6
Miscellaneous power (MW)	-17.0	-19.8	-24.3	-7.6	-9.1	-7.3
CO_2 capture power (MW)	-	-36.4	-55.0	-	-16.7	-29.0
Coal mass flow (kg/s)	43.2	50.4	37.9	19.3	23.1	18.5
System net power (MW)	698.7	618.7	539.8	309.0	284.7	264.0
Specific system power (kJ/kg)	1283.6	1136.6	991.7	1049.6	967.1	896.7
System net efficiency (%)	53.0	40.3	46.6	52.6	40.4	46.4

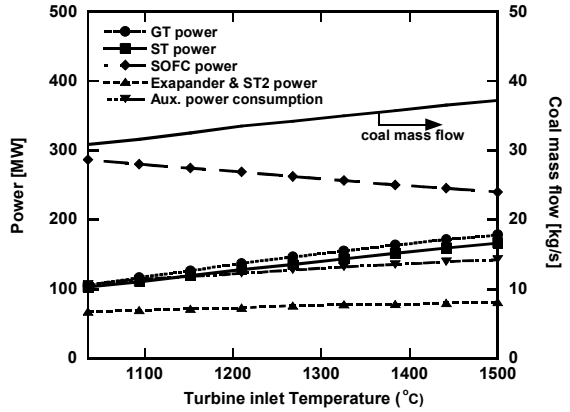

Fig. 6. Variations in power and coal mass flow with turbine inlet temperature (pressure ratio = 19.1): oxy-combustion system.

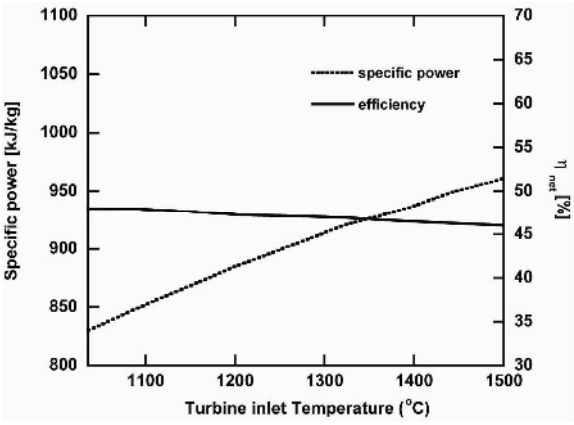

Fig. 7. Variations in net specific power and efficiency with turbine inlet temperature (pressure ratio =19.1): oxy-combustion system.

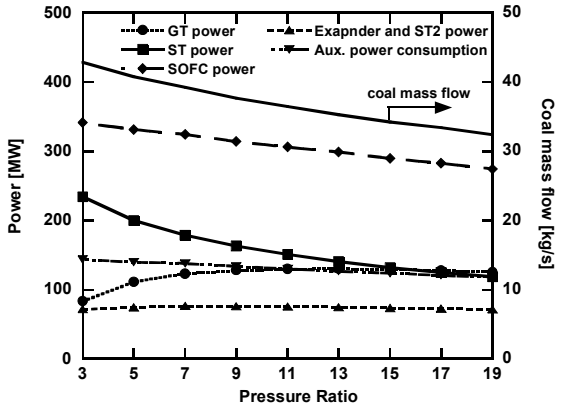

Fig. 8. Variations in power and coal mass flow with pressure ratio (turbine inlet temperature = 1145 °C): oxy-combustion system.

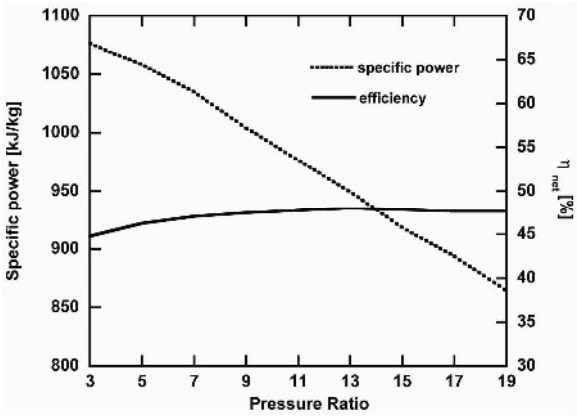

Fig. 9. Variations in net specific power and efficiency with pressure ratio (turbine inlet temperature = 1145 °C): oxy-combustion system.

(see Table 1 for the large difference in the turbine inlet temperatures of the two gas turbines). Even though the net specific power of the system using the E-class gas turbine is relatively lower, its net system efficiency is similar to that of the system using the G-class gas turbine. In other words, the net efficiency is almost insensitive to the selection of the gas turbine, which is very useful information.

To understand this result in a general way, we performed a parametric analysis of the oxy-combustion-based IG-SOFC/GT system by varying both the turbine inlet temperature and pressure ratio. In the G-class gas turbine, a large amount of syngas fuel should be supplied to the main combustor (gas turbine combustor) to achieve a turbine inlet temperature of 1500°C, which is much higher than the SOFC exit gas temperature of 900°C. However, in the E-class gas turbine, only a small amount of syngas fuel is required to be supplied to the combustor because of the relatively low turbine inlet temperature (1145°C). For example, in the oxy-combustion system, the ratio of syngas supplied to the gas turbine combustor to the total syngas is 33% and 7.6% for the G and E-class gas turbines, respectively. The two gas turbines have different pressure ratio as well.

The reference case for the parametric analysis was the oxy-combustion capture-based system using the G-class gas turbine. First, the pressure ratio was fixed and the effect of the turbine inlet temperature on system performance was examined. Figs. 6 and 7 show the results. Starting from the reference value of 1500°C, the reduction of the turbine inlet temperature was simulated by decreasing the syngas supply to the combustor. Steam cooling of the combustor was not included in this simulation because the E-class gas turbine does not use this scheme. Therefore, the results for the 1500 °C condition shown in Figs. 6 and 7 are slightly different from those for the G-class case shown in Table 2. A lower turbine inlet temperature reduces the syngas supply to the combustor (i.e., the total coal supply). As shown in Fig. 6, a reduction in turbine inlet temperature causes a decrease in gas turbine power. In addition, the resulting decrease in the turbine exit temperature of the gas turbine is negative with respect to steam turbine power production. The reduction of the total fuel supply with decreasing turbine inlet temperature also reduces the auxiliary power consumption. Variation in the

Table 3. Performance summary of IG-SOFC/GT systems: nitrogen supply to the SOFC.

	G-class gas turbine			E-class gas turbine		
CO_2 capture method	w/o capture	Pre-comb.	Oxy- comb.	w/o capture	Pre-comb.	Oxy-comb.
Gross power (MW)	849.3	847.1	732.2	378.6	387.6	356.2
GT power (MW)	300.7	311.7	174.7	96.8	99.1	56.8
Main ST power (MW)	262.3	164.7	182.2	102.0	57.8	78.6
Additional ST power (MW)	-	-	17.5	-	-	10.4
CO_2 expander power (MW)	-	-	71.3	-	-	30.7
SOFC power (MW)	286.3	370.7	286.6	179.8	230.7	179.7
Auxiliary power (MW)	-89.7	-147.4	-149.9	-39.9	-67.2	-70.1
ASU power (MW)	-71.6	-85.8	-62.7	-31.8	-39.1	-30.3
Miscellaneous power (MW)	-18.1	-21.7	-24.0	-8.1	-9.9	-9.1
CO_2 capture power (MW)	-	-39.9	-63.2	-	-18.3	-30.7
Coal mass flow (kg/s)	46.2	55.3	40.4	20.6	25.3	19.6
System net power (MW)	759.6	699.7	582.4	338.7	320.4	286.1
Specific system power (kJ/kg)	1395.5	1285.5	1070.0	1150.5	1088.3	971.8
System net efficiency (%)	53.9	41.4	47.2	53.9	41.5	47.8

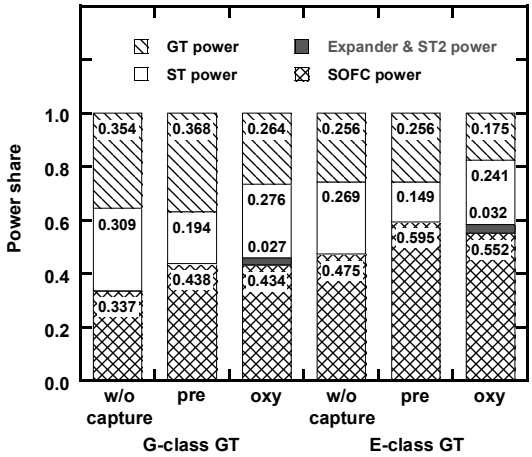

Fig. 10. Power share of IG-SOFC/GT system with nitrogen supply to the SOFC.

SOFC power showed a reversed trend; it increases with decreasing turbine inlet temperature. As the turbine inlet temperature decreases, the required turbine cooling air decreases, which increases the flow rate of the air supplied to the SOFC. As a result, more fuel can be supplied to the SOFC, generating more SOFC power output. Even with this SOFC power increase, the net system power decreases with deceasing turbine inlet temperature, as shown in Fig. 7. Since the reduction of the syngas supply to the combustor prevails over the increase of the syngas supply to the SOFC, the net coal supply also decreases with decreasing turbine inlet temperature. The two counteracting effects of decreases in both the net power output and the coal supply result in nearly constant net system efficiency.

Next, the impact of the gas turbine pressure ratio was examined, and Figs. 8 and 9 show the results. Here, the turbine inlet temperature was set to the temperature of the E-class gas turbine (1145°C) and the pressure ratio was varied. As the pressure ratio decreases, the compressor discharge temperature decreases. Accordingly, the gas flow recirculated from cathode exit to the inlet should be increased to meet the cathode inlet temperature. As a result, more syngas should be supplied to the fuel cell to satisfy the energy balance at the fuel cell, thereby increasing fuel cell power and auxiliary power consumption. The gas turbine power output is not very sensitive to the pressure ratio over a wide range, but decreases rather sharply as the pressure ratio decreases below 7. The steam turbine power increases with decreasing pressure ratio because the temperature and mass flow at the gas turbine exit increase. The net system performance variation is shown in Fig. 9. Because of the increase in fuel cell power and steam turbine power, the net specific power increases as the pressure ratio decreases. On the other hand, the system efficiency does not change significantly with pressure ratio because of the increase in coal supply with decreasing pressure ratio.

Examining the results of the two parametric analyses together, we concluded that the net system efficiency is not sensitive to the turbine inlet temperature or the pressure ratio, and the SOFC power share increases with decreasing turbine inlet temperature and pressure ratio. This is consistent with the result shown in Table 2 regarding the comparison between the systems using G-class and E-class gas turbines.

Additional comments on the influence of adding fuel to the gas turbine side (increasing turbine inlet temperature) are as follows. In many previously suggested SOFC/GT hybrid systems, the system efficiency was predicted to decrease rather dramatically as the additional fuel to the gas turbine side increases [33, 34]. This is because small gas turbines are much less efficient than SOFC and thus adding fuel to the gas turbine side definitely reduces the system efficiency. However, in the present study, the overall system is a combination between an SOFC and a gas turbine combined cycle (not a simple gas turbine). This is a key difference from the combination between an SOFC and a simple GT. Efficiencies of gas turbine combined cycles are comparable or even higher than SOFC

efficiency. It is clear that the combined cycle efficiency improves as the gas turbine performance enhances (e.g. from E to G-classes or from lower to higher turbine inlet temperature). Therefore, even if the fuel to gas turbine side is increased, the increased gas turbine combined cycle performance (power increase) nearly compensates for the fuel addition, resulting in an almost insensitive efficiency variation.

4.3 Influence of nitrogen supply location

In this section, we demonstrate the possibility of increasing system power output while keeping the compressor capacity (fixed air flow). It was done via modification of the two system layouts shown in Figs. 1 and 3. In the alternative layouts, the location of the supply of the nitrogen separated from the ASU in the power block was changed. The dotted lines indicated by ② represent the alternative layouts, and those indicated by ① represent the reference layouts. In the alternative layouts, nitrogen is mixed with the air flowing into the cathode instead of being supplied to the combustor. This design revision requires an increase of the SOFC cathode flow rate. In proportion to the increased cathode air flow, the fuel to the SOFC needs to be increased (therefore, the SOFC size increases) to operate the SOFC at the same temperature as in the reference case, which means that the entire system can be designed to produce more SOFC power output. Table 3 shows a design performance summary for the revised system layout, and Fig. 10 shows the power shares. The decrease in the oxygen concentration in the cathode due to the addition of nitrogen may affect the electrochemical performance, i.e. the voltage, of the cell stack. However, we did not consider such an effect because sufficiently reliable information on the voltage variation according to the nitrogen addition is not available. In comparison to the results given in Table 2, the SOFC power is higher in all system layouts. The net power was enhanced by 8 to 13% compared to the reference layouts. The net efficiency improved in all cases, as expected. The net efficiency did not change considerably but was turned out to increase slightly: about 1.1 percentage points enhancement on average.

5. Conclusion

The results of this study are summarized as follows.

(1) The effect of CO_2 capture on net performance was expected to be similar between the systems adopting G-class and E-class gas turbines. The oxy-combustion capture-based system was predicted to provide higher net efficiency than the pre-combustion capture cased system regardless of the choice of gas turbine.

(2) With a relatively low performance gas turbine (E-class), the power shares of the gas turbine and the steam turbine are lower in comparison to a high performance gas turbine (G-class). Although the net specific power of the system using the E-class gas turbine is lower, the net system efficiency is quite similar to that of the system using the G-class gas turbine. From parametric analysis, we found that the net system efficiency is not sensitive to the turbine inlet temperature or the pressure ratio, which explains the similar net efficiencies between the systems using the two gas turbines with very different specifications. In particular, even if the fuel to gas turbine side increases, the increased gas turbine combined cycle performance nearly compensates for the fuel addition, resulting in an almost insensitive efficiency variation.

(3) The power capacity of the IG-SOFC/GT system can be increased by supplying nitrogen separated from the ASU to the SOFC instead of the gas turbine combustor. The net system power output was predicted to increase by 8 to 13% depending on the system layout. The net efficiency did not change considerably: a slight increase was estimated.

Acknowledgment

This research was supported by Basic Science Research Program through the National Research Foundation of Korea (NRF), funded by the Ministry of Education, Science and Technology (no. 2012-001443).

Nomenclature

ASU : Air separation unit
BAC : Booster air compressor
CGSU : Cold gas cleanup unit
CCU : Carbon dioxide capture unit
CSU : Carbon dioxide separation unit
F : Faraday constant (96,486 J/Vmol)
GT : Gas turbine
HHV : Higher heating value (kJ/kg)
IGCC : Integrated gasification combined cycle
IG-SOFC/GT : Integrated gasification SOFC/GT cycle
ITM : Ion transport membrane
MAC : Main air compressor
$\dot{m}$: Mass flow rate (kg/s)
$\dot{n}$: Molar flow rate (kmol/s)
P : Pressure (kPa)
R : Gas constant (8.314 kJ/kmol K)
SOFC : Solid oxide fuel cell
T : Temperature (^oC)
V : Voltage (V)
ΔV : Voltage rise (V)
WGS : Water-gas shift reactor
$\dot{W}$: Power (MW)
η : Efficiency

Subscripts

aux : Auxiliary
C : Compressor
CC : Carbon dioxide capture
conv : Conversion

DC : Direct current
exp : Expander
gen : Generator
HP : High pressure
IP : Intermediate pressure
j : Compression stage
LP : Low pressure
m : Mechanical
misc : Miscellaneous
mo : Motor
P : Pump
ref : Reference
S : Separator
ST : Steam turbine
ST2 : Additional steam turbine
T : Turbine

References

[1] J. J. Lee, Y. S. Kim, K. S. Cha, T. S. Kim, J. L. Sohn and Y. J. Joo, Influence of system integration options on the performance of an integrated gasification combined power plant, *Applied Energy*, 86 (2009) 1788-1796.

[2] E. O. Oluyede and J. N. Phillips, Fundamental impact of firing syngas in gas turbines, *ASME paper*, 2007-27385 (2007).

[3] Y. S. Kim, J. J. Lee, T. S Kim, J. L. Sohn and Y. J. Joo, Performance analysis of a syngas-fed gas turbine considering the operating limitations of its components, *Applied Energy*, 87 (2010) 1602-1611.

[4] Y. S. Kim, J. J. Lee, T. S. Kim and J. L. Sohn, Effects of syngas type on the operation and performance of a gas turbine in integrated gasification combined cycle, *Energy Conversion and Management*, 52 (2011) 2262-2271.

[5] R. A. Dennis and R. Harp, Overview of the U.S. department of energy's office of fossil energy advanced turbine program for coal based power systems with carbon capture, *ASME paper* GT2007-28338 (2007).

[6] M. Kanniche and C. Bouallou, CO_2 capture study in advanced integrated gasification combined cycle, *Applied Thermal Engineering*, 27 (2007) 2693-2702.

[7] C. Descamps, C. Bouallou and M. Kanniche, Efficiency of an integrated gasification combined cycle (IGCC) power plant including CO_2 removal, *Energy*, 33 (2008) 847-881.

[8] M. C. Williams, J. P. Strakey and W. Sudoval, US DOE fossil energy fuel cells program, *J. of Power Sources*, 159 (2006) 1241-1247.

[9] J. F. Pierre. Office of fossil energy fuel cell program FY2007 annual report (2007) 3-5.

[10] S. E. Veyo, S. D. Vora, K. P. Litzinger and W. L Lundberg, Status of pressurized SOFC/gas turbine power system development at Siemens Westinghouse, *ASME paper* GT-2002-30670 (2002).

[11] E. Liese. Comparison of pre-anode and post-anode carbon dioxide separation for IGFC system, *ASME paper* GT2009-59144 (2009).

[12] M. C. Romano, S. Campanari, V. Spallina and G. Lozza, SOFC-based hybrid cycle integrated with a coal gasification plant, *ASME paper* GT2009-59551 (2009).

[13] M. Li, A. D Rao, J. Brouwer and G. S. Samuelsen, Design of highly efficient coal-based integrated gasification fuel cell power plants, *J. of Power Sources*, 195 (2010) 5707-5718.

[14] S. K. Park, J. H. Ahn and T. S Kim, Performance evaluation of integrated gasification solid oxide fuel cell/gas turbine systems including carbon dioxide capture, *Applied Energy*, 88 (2011) 2976-2987.

[15] J. Gibbins and H. Chalmers, Carbon capture and storage, *Energ Policy*, 36 (2008) 4317-4322.

[16] M. Kanniche, R. Gros-Bonnivard, P. Jaud, J. Valle-Marcos, J. M. Amann and C. Bouallou, Pre-combustion, post-combustion and oxy-combustion in thermal power plant for CO_2 capture, *Applied Thermal Engineering*, 30 (2010) 53-62.

[17] W. Sanz, H. Jericha, B. Bauer and F. Gottlich, Qualitative and quantitative comparison of two promising oxy-fuel power cycles for CO_2 capture. *J. of Engineering for Gas Turbines and Power*, 130 (2008) 031702-1-11.

[18] R. E. Anderson, S. MacAdam, F. Viteri, D. O. Davies, J. P. Downs and A. Paliszewski. Adapting gas turbines to zero emission oxy-fuel power plants, *ASME paper* GT2008-51377 (2008).

[19] S. H. Tak, S. K. Park, T. S. Kim, J. L. Sohn and Y. D. Lee, Performance analyses of oxy-fuel power generation systems including CO_2 capture: comparison of two cycles using different recirculation fluids, *J. of Mechanical Schience and Technology*, 24 (2010) 1947-1954.

[20] H. J. Yang, D. W. Kang, J. H Ahn and T. S. Kim, Evaluation of design performance of the semi-closed oxy-fuel combustion combined cycle, *ASME paper* GT2012-69141 (2012).

[21] V. White, P. Armstrong and K. Fogash, Oxygen supply for oxyfuel CO_2 capture, *Proc. of the 1st Oxyfuel Combustion Conference*, Cottbus, Germany (2009).

[22] S. K. Park, T. S Kim, J. L. Sohn and Y. D. Lee, An integrated power generation system combining solid oxide fuel cell and oxy-fuel combustion for high performance and CO_2 capture, *Applied Energy,* 88 (2011) 1187-1196.

[23] P. N. Dyer, R. S. L. Russek and D. M Taylor, Ion transport membrane technology for oxygen separation and syngas production, *Solid State Ionics,* 134 (2000) 21-33.

[24] C. M. Chen, D. L. Bennett, M. F. Carolan, E. P. Poster, W. L. Schinsk and D. M. Taylor, *ITM syngas ceramic membrane technology for synthesis gas production*, In : Bao X, Xu Y, editor. Studies in Surface Science and Catalysis, Elsevier, 147 (2004) 50-55.

[25] J. Tennant, S. Maley and D. Bennett, Development of ion transport membrane (ITM) oxygen technology for integration in IGCC and other advanced power generation systems, *NETL report 2011*:FT40343 (2011).

[26] Aspen Technology, *AspenOne HYSYS, ver. 2006.5*, Aspen Technology, Inc. (2007).
[27] W. Shelton and J. Lyons, Shell gasifier IGCC base cases. *NETL report 1998*: PED-IGCC-98-002 (1998).
[28] J. M. Amann, M. Kanniche and C. Bouallos, Natural gas combined cycle power plant modified into an O_2/CO_2 cycle for CO_2 capture, *Energy Conversion and Management*, 50 (2009) 510-521.
[29] M. K. Julianne, Cost and performance baseline for fossil energy plants, *NETL report 2007*: DOE/NETL-2007; 1281 (2007).
[30] J. Larminie and A. Dicks, *Fuel cell systems explained*, Second Ed, John Wiley & Sons, Chichester (2003) 35-41.
[31] R. Farmer, *2007-08 Gas turbine world handbook*, Pequot Publishing Inc (2008) 26.
[32] I. Diakunchak and H. J Kiesow. The history of the Siemens gas turbine, *ASME paper* GT2008-50507(2008).
[33] W. J. Yang, S. K. Park, T. S. Kim, J. H. Kim, J. L. Sohn and S. T. Ro, Design performance analysis of pressurized solid oxide fuel cell/gas turbine hybrid systems considering temperature constraints, *Journal of Power Sources*, 160 (2006) 462-473.
[34] S. K. Park and T. S. Kim, Comparison between pressurized design and ambient pressure design of hybrid solid oxide fuel cell-gas turbine systems, *Journal of Power Sources*, 163 (2006) 490-499.

J. H. Ahn received his M.S. degree from Dept. of Mechanical Engineering, Inha University in 2012. His major research topic is performance analysis of energy systems, especially power plants with carbon capture.

Sung Ku Park received his Ph.D. degree from Dept. of Mechanical Engineering, Inha University in 2011, and is now a researcher at IGCC team, Corporate R&D Institute, DOOSAN Heavy Industries & Construction Co., LTD, Korea.

T. S. Kim received his Ph.D. degree from Dept. of Mechanical Engineering, Seoul National University in 1995. He has been with Dept of Mechanical Engineering, Inha University since 2000. His research interests are design and analysis of advanced energy systems including gas/steam turbine based power plants.